Signal Processing 90 (2010) 173–179

Contents lists available at ScienceDirect

Signal Processing

journal homepage: www.elsevier.com/locate/sigpro

Modified ESPRIT (M-ESPRIT) algorithm for time delay estimation in both any noise and any radar pulse context by a GPR radar

Cédric Le Bastard [a,*], Vincent Baltazart [b], Yide Wang [c]

[a] Laboratoire Régional des Ponts et Chaussées (LRPC), ERA 17, BP 69, F-49136 Les Ponts-de-Cé, France
[b] Laboratoire Central des Ponts et Chaussées (LCPC), BP 4129, F-44341 Bouguenais cedex, France
[c] IREENA, Ecole Polytechnique de l'Université de Nantes, BP 50609, F-44306 Nantes cedex 3, France

ARTICLE INFO

Article history:
Received 24 July 2008
Received in revised form
13 February 2009
Accepted 8 June 2009
Available online 13 June 2009

Keywords:
Time delay estimation (TDE)
Non-destructive testing and evaluation (NDTE)
Radar
Resolution

ABSTRACT

This paper presents M-ESPRIT, a modified version of the ESPRIT algorithm, for the purpose of time delay estimation of backscattered radar signals. The proposed algorithm takes both the transmitted pulse shape and any noise into account. It can process raw data from experimental device without the preprocessing which would be required with the conventional ESPRIT algorithm.

1. Introduction

Among subspace algorithms, ESPRIT affords a direct parameter estimation with a lower computational load. It has been originally formulated for array signal processing [1]. An extension of the algorithm has been proposed in [2] to deal with any array geometry in additive white Gaussian noise. In this paper, we use the ESPRIT algorithm for the purpose of time delay estimation (TDE) of overlapping radar echoes in order to measure the thicknesses of a stratified medium.

The application of the conventional ESPRIT algorithm to TDE assumes an ideal data model composed of time-shifted Dirac pulses [3]. Thus, a whitening step of data by the radar pulse is needed before applying the conventional ESPRIT technique. As pointed out by different authors (e.g. [4]), this preprocessing operation modifies the properties of noise and may degrade the signal to noise ratio (SNR) of the largest echoes.

Two extensions of the ESPRIT algorithm have been proposed for TDE, called for convenience in this paper E-ESPRIT and F-ESPRIT, respectively. E-ESPRIT in [3] can handle the colored noise but suppose an ideal radar pulse. F-ESPRIT in [5] takes into account the radar pulse but suppose a temporally white Gaussian noise.

This paper aims at generalizing these latter works by taking both the radar pulse shape and any noise into account. As a result, the generalized version of the ESPRIT algorithm, called M-ESPRIT (modified ESPRIT), can directly process the radar raw data without any preprocessing.

In the next section, we present the radar data model used in this paper. Section 3 presents the proposed M-ESPRIT algorithm. Simulation results comparing M-ESPRIT with the E-ESPRIT, the F-ESPRIT and the conventional ESPRIT algorithms are provided in Section 4, and the paper concludes in Section 5.

* Corresponding author. Tel.: +33 2 41 79 13 05; fax: +33 2 41 44 32 76.
E-mail addresses: cedric.lebastard@developpement-durable.gouv.fr (C. Le Bastard), vincent.baltazart@lcpc.fr (V. Baltazart), Yide.wang@univ-nantes.fr (Y. Wang).

0165-1684/$ - see front matter © 2009 Elsevier B.V. All rights reserved.
doi:10.1016/j.sigpro.2009.06.007

2. Data model for TDE

To measure the thickness of a stratified medium by a radar, backscattered signals from $K-1$ layers which are assumed to be horizontal, homogeneous, roughless and non-dispersive at the usual radar frequency wavelengths are to be processed. In most cases (e.g. [6,8]), radar data are processed on a scan-by-scan basis to provide the depth structure of the medium from the time delays associated with each layer and the wave speed therein. Therefore, the received signal is one dimensional and consists of the sum of K time-shifted and attenuated replicas of the transmitted radar pulse $e(t)$.

For applying spectral analysis techniques to time delay estimation, the received signal is usually formulated in the frequency domain [9]. Considering N equispaced frequency samples f_n within the bandwidth B, the $(N\times 1)$ received signal vector $\mathbf{y}$ can be written as follows [6]:

$$\mathbf{y}=\mathbf{\Lambda A c}+\mathbf{n} \tag{1}$$

where $\mathbf{A}$ is the $(N\times K)$ mode matrix, composed of the K steering vectors $\mathbf{a}(T_k)=[e^{-2j\pi f_1 T_k},e^{-2j\pi f_2 T_k},\ldots,e^{-2j\pi f_N T_k}]^T$ of size $(N\times 1)$ as columns, with $k=1,2,\ldots,K$, $\mathbf{\Lambda}$ is the $(N\times N)$ diagonal matrix whose diagonal elements are the Fourier transform $\tilde{e}(f)$ of the radar pulse $e(t)$, $\mathbf{c}$ is the $(K\times 1)$ vector of echoes amplitudes and $\mathbf{n}$ is the $(N\times 1)$ zero mean noise vector.

Different simplifications can be made on the basis of (1). For example, if the matrix $\mathbf{\Lambda}$ is equal to the $(N\times N)$ identity matrix and the vector $\mathbf{n}$ is a white Gaussian uncorrelated noise vector, (1) is simplified to the ideal data model used by the conventional ESPRIT algorithm when applied to TDE.

As for the other subspace algorithms, ESPRIT makes use of the eigenstructure of the covariance matrix to perform TDE [1,3]. According to model (1) and assuming noise to be independent with the echoes, the covariance matrix $\mathbf{\Gamma_y}$ can be written as

$$\mathbf{\Gamma_y}=E[\mathbf{yy}^H]=\mathbf{\Gamma}_{sig}+\sigma^2\mathbf{\Sigma}_o \tag{2}$$

where $E[\cdot]$ denotes the ensemble average, and $\mathbf{\Gamma}_{sig}$ and $\mathbf{\Sigma}_o$ are the covariance matrices of the signal and noise, respectively.

The covariance matrix of noise $\mathbf{\Sigma}_o$ has been normalized according to [10] such that $\mathrm{tr}(\mathbf{\Sigma}_o)=N$. The latter matrix is reduced to the $(N\times N)$ diagonal matrix under the uncorrelated noise assumption.

The covariance matrix of the signal $\mathbf{\Gamma}_{sig}$ is expressed according to data model (1) as follows:

$$\mathbf{\Gamma}_{sig}=\mathbf{\Lambda A\Gamma_c A}^H\mathbf{\Lambda}^H \tag{3}$$

where $\mathbf{\Gamma_c}$ is the $(K\times K)$ dimensional covariance matrix of the source vector $\mathbf{c}$.

According to [3], from the generalized singular value decomposition (GSVD) of the covariance matrix $\mathbf{\Gamma}_y$, we have

$$\mathbf{\Gamma}_{sig}\mathbf{V}_{sig}=\mathbf{\Sigma}_o\mathbf{V}_{sig}\mathbf{G} \tag{4}$$

with

$$\mathbf{G}=\mathbf{D}_{sig}-\sigma^2\mathbf{I}_{K\times K} \tag{5}$$

where the generalized eigenvectors $\mathbf{v}_k$ associated with the signal subspace are arranged in the matrix $\mathbf{V}_{sig}$ as columns, and the corresponding generalized eigenvalues λ_k are the diagonal elements of matrix $\mathbf{D}_{sig}$ and σ^2 is the smallest generalized eigenvalue of the noise subspace.

3. Generalized ESPRIT (M-ESPRIT) for TDE

In this section, the ESPRIT algorithm is generalized and developed for the data model in Eq. (1) by taking account of both the radar pulse shape and any noise covariance matrix. We call this algorithm as modified ESPRIT (M-ESPRIT) as opposed to the previously mentioned algorithms (i.e. E- and F-ESPRIT) which require some preprocessing procedures to recover either the white noise or the ideal radar pulse structure. Note that if $\mathbf{\Lambda}=\mathbf{I}_{N\times N}$ and $\mathbf{\Sigma}_o=\mathbf{I}_{N\times N}$, we are in the same situation of application of the conventional ESPRIT algorithm.

For TDE, the ESPRIT algorithm divides the data vector $\mathbf{y}$ into two overlapping data sub-bands. Sub-bands comprise $N-1$ samples and overlap with each other by $N-2$ samples. The $((N-1)\times K)$ dimensional mode matrices corresponding to each sub-band, $\mathbf{A}_1$ and $\mathbf{A}_2$, are related to each other by the following $(K\times K)$ diagonal matrix $\mathbf{\Phi}$, whose elements depend on the time delay to be estimated:

$$\mathbf{A}_2=\mathbf{A}_1\mathbf{\Phi} \tag{6}$$

$$\text{with: } \mathbf{\Phi}=diag(e^{-2i\pi\Delta f T_1},\ldots,e^{-2i\pi\Delta f T_K}) \tag{7}$$

Because the matrix $\mathbf{\Phi}$ cannot be estimated from data, ESPRIT further exploits the linear relation in (6) within the GSVD of the data covariance matrix in (4). In the Appendix, it is shown that the time delays T_k can be retrieved from the eigenvalues of the matrix $\mathbf{K}$, defined as

$$\mathbf{\Sigma}_{o,2}\mathbf{V}_{sig}=(\mathbf{\Lambda}_2\mathbf{\Lambda}_1^{-1}\mathbf{\Sigma}_{o,1}\mathbf{V}_{sig})\mathbf{K} \tag{8}$$

where $\mathbf{\Sigma}_{o,j}$ $(j=1,2)$ are two overlapping sub-band matrices of size $((N-1)\times N)$, which are defined as the $N-1$ upper lines and the $N-1$ lower lines of the noise covariance matrix $\mathbf{\Sigma}_o$, respectively, according to

$$\mathbf{\Sigma}_o=\begin{pmatrix}-\\ \mathbf{\Sigma}_{o,2}\end{pmatrix}=\begin{pmatrix}\mathbf{\Sigma}_{o,1}\\ -\end{pmatrix} \tag{9}$$

and $\mathbf{\Lambda}_j$ $(j=1,2)$ are two $((N-1)\times(N-1))$ diagonal matrices defined from the pulse radar matrix $\mathbf{\Lambda}$ as

$$\mathbf{\Lambda}_j=diag(\tilde{e}(f_j),\tilde{e}(f_{j+1}),\ldots,\tilde{e}(f_{N-2+j})) \tag{10}$$

Then, two ways can be used to calculate the matrix $\mathbf{K}$ from (8). At first, the least squares (LS) solution can be readily obtained from (8) as follows:

$$\mathbf{K}_{LS}=(\mathbf{\Psi}_{sig,1}^H\mathbf{\Psi}_{sig,1})^{-1}\mathbf{\Psi}_{sig,1}^H\mathbf{\Omega}^{-1}\mathbf{\Psi}_{sig,2} \tag{11}$$

where the two following matrices are introduced to simplify the mathematical notations:

$$\mathbf{\Psi}_{sig,j}=\mathbf{\Sigma}_{o,j}\mathbf{V}_{sig} \tag{12}$$

$$\mathbf{\Omega}=\mathbf{\Lambda}_2\mathbf{\Lambda}_1^{-1}=diag\left(\frac{\tilde{e}(f_2)}{\tilde{e}(f_1)},\ldots,\frac{\tilde{e}(f_N)}{\tilde{e}(f_{N-1})}\right) \tag{13}$$

From (12) and (13), we can observe that the matrices $\mathbf{\Psi}_{sig,j}$ $(j=1$ or $2)$ deal with the modification of the signal

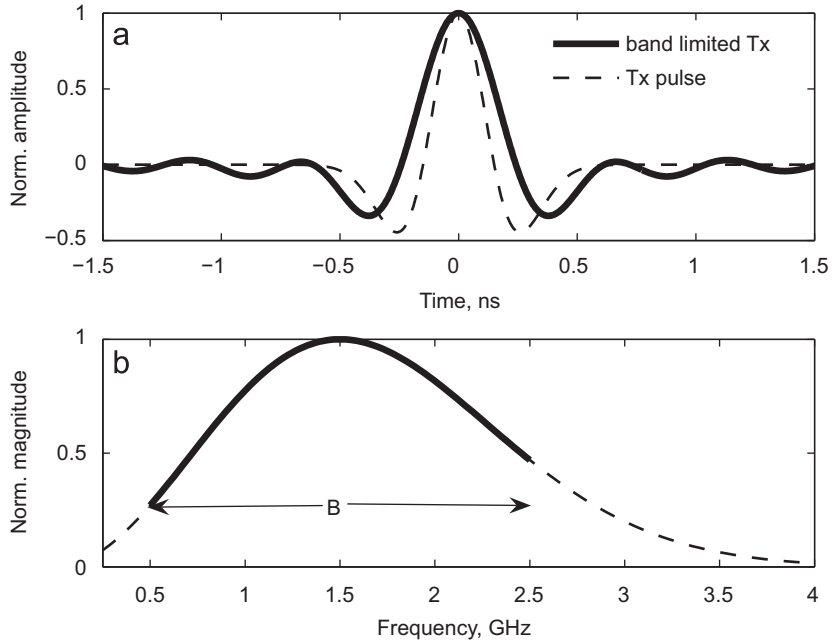

Fig. 1. Time (a) and frequency (b) signatures of the simulated radar pulse (ricker type); solid lines present the data to be processed within the frequency bandwidth $B = 2$ GHz, while dashed lines present the data from unbounded bandwidth.

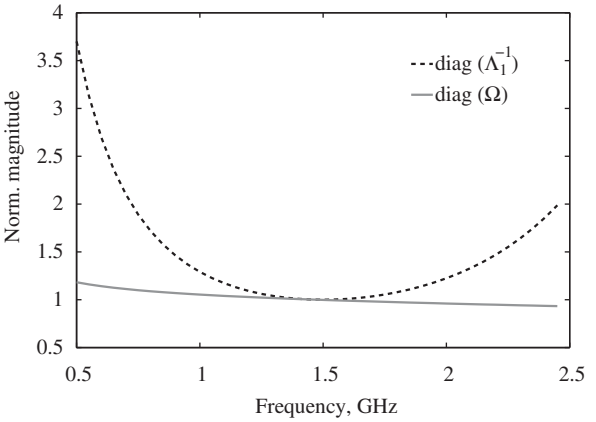

Fig. 2. Diagonal elements of matrices $\mathbf{\Omega}$ and $\mathbf{\Lambda}_1^{-1}$ when the radar pulse is a ricker pulse defined in Fig. 1.

subspace due to the noise metric, and $\mathbf{\Omega}$ takes the radar pulse shape into account. In this application, the GPR pulse shape commonly used is ricker pulse, which is defined as the second derivative of a Gaussian pulse [11]. In the frequency domain, the magnitude of $\tilde{e}(f)$ shows smooth variations with no zero occurrence within a large frequency bandwidth as shown in Fig. 1. The variations of diagonal elements of matrices $\mathbf{\Omega}$ and $\mathbf{\Lambda}_1^{-1}$ are depicted in Fig. 2. We observe from this figure that the values of $\mathbf{\Omega}$ within the frequency bandwidth are close to one and show smaller dynamic range than matrix $\mathbf{\Lambda}^{-1}$ does. Then, the discrepancy which is due to the whitening of data by the radar pulse may still exist but with a smaller degradation of the SNR of the largest echoes.

Secondly, the total least square (TLS) solution for the matrix $\mathbf{K}$ in (8) requires to perform the GSVD of the couple of matrices $[\mathbf{\Psi}_{sig,2}, \mathbf{\Omega}\mathbf{\Psi}_{sig,1}]$. The higher computational load would be justified by an improved robustness of the solution especially at low SNR [12].

Further simplifications can be made if the noise covariance matrix is diagonal, i.e. $\mathbf{\Sigma}_o = diag(\sigma_1^2, \sigma_2^2, \ldots, \sigma_N^2)$. Under this condition, (8) is simplified to

$$\mathbf{V}_{sig,2} = \mathbf{\Omega}_\Sigma \mathbf{V}_{sig,1}\mathbf{K} \tag{14}$$

where $\mathbf{\Omega}_\Sigma$ is defined as

$$\mathbf{\Omega}_\Sigma = diag\left(\frac{\sigma_1^2}{\sigma_2^2}\frac{\tilde{e}(f_2)}{\tilde{e}(f_1)}, \ldots, \frac{\sigma_{N-1}^2}{\sigma_N^2}\frac{\tilde{e}(f_N)}{\tilde{e}(f_{N-1})}\right) \tag{15}$$

and the two sub-matrices $\mathbf{V}_{sig,1}$ and $\mathbf{V}_{sig,2}$ are defined below as the $N-1$ upper lines and the $N-1$ lower lines of $\mathbf{V}_{sig}$, respectively,

$$\mathbf{V}_{sig} = \begin{pmatrix} - \\ \mathbf{V}_{sig,2} \end{pmatrix} = \begin{pmatrix} \mathbf{V}_{sig,1} \\ - \end{pmatrix} \tag{16}$$

For ESPRIT-type algorithms, the overall computational load is principally determined by the eigenvalue decomposition of the data covariance matrix in Eq. (2). This step includes $O(N^3)$ complex multiplications and is required for the four mentioned algorithms (i.e. conventional ESPRIT, E-ESPRIT, F-ESPRIT and M-ESPRIT). Therefore, the computational load has been found to be roughly the same for the four algorithms, which is verified by our simulations.

4. Computer and experimental tests

In this section, we present some computer and experimental results and we compare the performance of the proposed method (M-ESPRIT) with the three mentioned algorithms (conventional ESPRIT, E-ESPRIT by [3] and F-ESPRIT by [5]). A simple modification of E-ESPRIT is also introduced to enable further comparison with M-ESPRIT.

4.1. Numerical results

These simulations have been carried out for the thickness measurement of a stratified medium.

The performance has been established by a Monte Carlo process, which consists of 500 independent runs (U) of algorithms. For each run, the covariance matrix is estimated from 200 independent snapshots. To analyze the influence of the radar pulse and that of the noise, the simulations are carried out with a noise whose covariance matrix is non-diagonal.

The performance has been derived from both the time resolution capability and the root mean square error (RMSE) on the estimated thickness. RMSE is conventionally used to assess the performance in parameter estimation. However, it has been found more useful to provide the end-user with the relative RMSE (RRMSE) on the thickness, which is defined as follows:

$$RRMSE\ [\%] = 100 \times \frac{\sqrt{\frac{1}{U}\sum_{j=1}^{U}(\hat{e}_j - e)^2}}{e} \tag{17}$$

where $\hat{e}_j$ denotes the estimated thickness for jth run of algorithms and e the true value. The performance of algorithms is considered as reasonably good when RRMSE is below 5% [6]. The time resolution is defined hereafter as the $B\Delta\tau$ product, where B is the frequency bandwidth of the radar device and $\Delta\tau$ is the smallest differential time shift between echoes distinguishable by the processing. To suit the application in [6], $B\Delta\tau$ must remain smaller than 0.6 for a 2 GHz radar bandwidth.

The four ESPRIT algorithms (i.e. conventional, E-, F- and M-) are performed on the data model (1) with only two echoes (i.e. $K = 2$). In order to determine the best performance and limitation of algorithms, two further favorable conditions have been assumed in the simulations: the signal subspace rank is equal to the expected number of echoes, i.e. 2, and the null correlation between echoes is assumed.

The radar pulse $e(t)$ is a ricker pulse, as shown in Fig. 1. The parameters of the pulse have been chosen in accordance with the characteristics of conventional GPR: the central frequency is $f_0 = 1.5$ GHz and the bandwidth B is limited to 2 GHz.

The data set is composed of 41 equispaced frequency samples within a 2 GHz bandwidth. The SNR has been fixed with respect to the first arrival signal (i.e. the echo from the interface at the top). Due to larger permittivity of the layer underneath, the second echo has a smaller magnitude; it has been fixed to −6 dB with respect to the first echo. To determine the limitation in resolution capability, different data sets have been generated by varying the thickness from 1.7 to 67 mm, such that the corresponding $B\Delta\tau$ product spans the interval [0.05, 2].

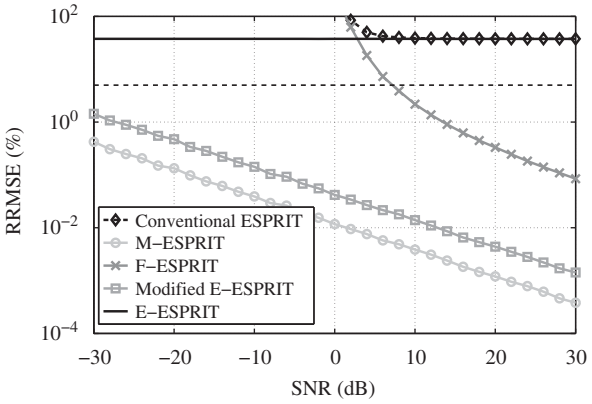

Fig. 3. RRMSE variation on estimated thickness vs. SNR after 500 Monte Carlo simulations; $B\Delta\tau = 0.6$; uncorrelated echoes; dotted line shows the 5% RRMSE threshold.

Fig. 3 represents RRMSE variation on estimated thickness vs. SNR for overlapping echoes (with $B\Delta\tau = 0.6$). We observe at first that the RRMSE increases continuously with decreasing SNR for any algorithm. M-ESPRIT delivers the best performance for any SNR. Contrary to the latter, a bias is observed on TDE with the conventional ESPRIT, the original version of E-ESPRIT and F-ESPRIT, because these algorithms do not account for either the radar pulse or the noise metric. The error on the noise metric for F-ESPRIT shows the most influence at low SNR. F-ESPRIT tends to provide reliable performance at medium to high SNR, depending on the $B\Delta\tau$ product. To support further comparison with M-ESPRIT, E-ESPRIT has been applied after the data whitening by the radar pulse. The latter version is called thereafter modified E-ESPRIT. This modification of the original algorithm proposed in [3] strongly improves the performance which tends to come close to that of M-ESPRIT. Furthermore, the comparison between both algorithms shows that it is better to perform M-ESPRIT on raw data (i.e. with the radar pulse accounted for in the steering vector) rather than modified E-ESPRIT (i.e. the radar pulse accounted for in the noise metric).

The resolution performance of the algorithms is shown in Fig. 4 with regards to the time resolution at low SNR, i.e. 0 dB. RRMSE increases continuously with decreasing $B\Delta\tau$ product. The vertical dotted line at 0.6 figures the time resolution threshold suited to the application in [6]. A systematic error (bias) is expected for the conventional ESPRIT, the E- and F-ESPRIT algorithms because either the radar pulse and/or the noise metric are not accounted for in the algorithms. The relative RMSE may then be found superior to 100%. At this SNR, the conventional ESPRIT and the E-ESPRIT algorithms are worthless because they cannot offer high resolution capability within the application: the RRMSE falls below 5% for $B\Delta\tau$ larger than one. Only the M-ESPRIT and the modified E-ESPRIT methods have acceptable performance. M-ESPRIT shows the best resolution capability and the best accuracy, followed by

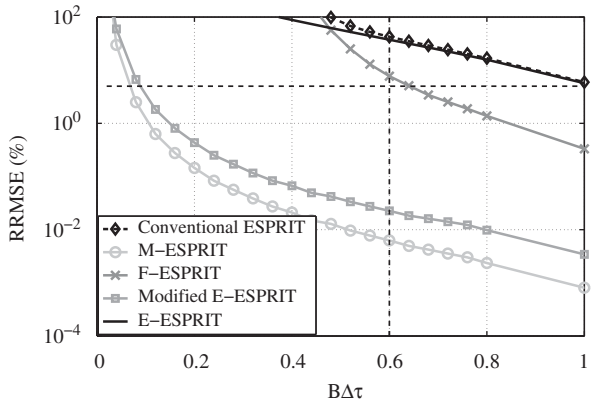

Fig. 4. RRMSE variation on estimated thickness vs. $B\Delta\tau$ product after 500 Monte Carlo simulations; SNR = 0 dB; uncorrelated echoes; horizontal and vertical dotted lines show the 5% RRMSE and the 0.6 resolution power thresholds, respectively; the application criterion in [6] is satisfied when the performance of algorithms falls into the lower left part of the dotted lines.

the modified E-ESPRIT. Moreover, unlike M-ESPRIT, a whitening step of preprocessing is necessary for modified E-ESPRIT. Simulation results show the improvement in estimation performance provided by taking into account the radar pulse into the steering vector rather than into the noise metric.

4.2. Experiments: preliminary results

The performance of the algorithms has been tested in the laboratory on roughless materials. The wideband exponential tapered slot antenna (ETSA) in [7] has been used and combined with a broad band vector network analyzer (VNA) to provide a step-frequency radar. The antenna was raised above the surface to insure to collect backscattering data at nadir and in far field conditions accordingly to the data model in Eq. (1). VNA guarantees a high SNR level and provides monostatic recording conditions. The calibration procedure detailed in [13] and the time filtering procedure allow to filter the transient signal and to select only the useful signal part, which is composed of the backscattered echoes from the two interfaces. The experimental device shown in Fig. 5 is expected to provide data which closely obey to the signal model in Section 4.1. The data set consists in a collection of backscattered data at different heights above a metallic plate $0.6 \times 0.6\,\mathrm{m}^2$. Denoting $y_1(f)$ and $y_2(f)$ as the backscattered data from the metallic plate at two heights h_1 and h_2, respectively, the sum $y(f) = y_1(f) + y_2(f)$ may represent the signal from a virtual two-layer medium filled in with air. The layer thickness then equals the height difference $h_2 - h_1$.

In addition to that, the data set enables to vary the cross-correlation amplitude between echoes. The full correlation case is obtained by computing the covariance matrix $\hat{\mathbf{\Gamma}}_y^{hc}$ attached to the sum $y_1(f) + y_2(f)$. In contrast, the null correlation matrix $\hat{\mathbf{\Gamma}}_{\mathbf{y}}^{nc}$ is formed from the sum of the covariance matrices of the data attached to different heights. Both matrices are then defined as

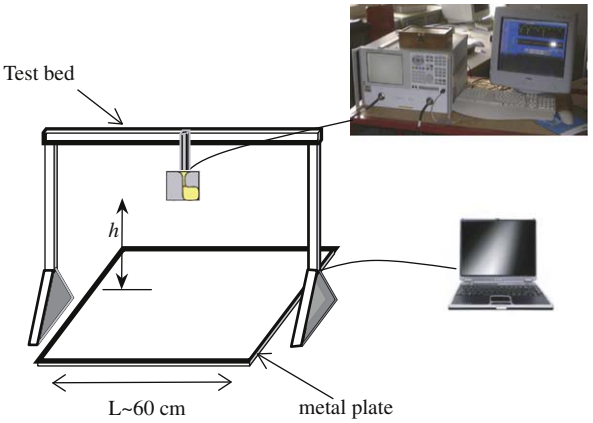

Fig. 5. Scheme of the experimental device with step-frequency radar.

follows:

$$\hat{\mathbf{\Gamma}}_{\mathbf{y}}^{hc} = \langle (\mathbf{y}_1 + \mathbf{y}_2) \times (\mathbf{y}_1 + \mathbf{y}_2)^H \rangle \tag{18}$$

$$\hat{\mathbf{\Gamma}}_{\mathbf{y}}^{nc} = \langle \mathbf{y}_1 \mathbf{y}_1^H \rangle + \langle \mathbf{y}_2 \mathbf{y}_2^H \rangle \tag{19}$$

In the situation where the backscattered echoes are highly correlated to each other, the rank of the source correlation matrix is less than the number of echoes, which results in failure of the ESPRIT algorithm. To alleviate this problem and to recover a full rank matrix, the covariance matrix may be estimated using either the well-known spatial smoothing process (SSP)/modified SSP (MSSP) averaging techniques [14] or the newer smoothing technique DEcomposition de l'Espace Source Estimé (DEESE) in [15]. Both techniques show the same performance for a large amount of data, but with heavier computer load for DEESE [15]. The SSP/MSSP averaging techniques have been studied in [6] within the scope of thickness measurement. It was shown that an optimized parametering of the MSSP technique enables to achieve the best performance of algorithms, i.e. when the echoes are uncorrelated. Thereafter, only the null correlation case is discussed. The covariance matrix $\hat{\mathbf{\Gamma}}_{\mathbf{y}}^{nc}$ is estimated from an average over 100 independent snapshots of data $y_{1,2}(f)$ recorded at the same location above the metallic plane. Each snapshot is made of 281 frequency samples equispaced by 10 MHz within the $B = 2.8$ GHz bandwidth, around a central frequency of 3.2 GHz. The $B\Delta\tau$ product, with B fixed, changes with the difference between the two heights of the metallic plane ($\Delta h = c\Delta\tau/2$, with c the celerity).

Four different heights have been selected for the data set. The lowest height satisfy nevertheless the far field conditions for the ETSA antenna. We get a height shift Δh of 2.25, 4.5 and 6.75 cm. The corresponding differential time delays between echoes ($\Delta\tau$) are equal to 0.15, 0.3 and 0.45 ns, respectively. In order to ease the calibration stage and to get the signal in one step, the signal to be processed is generated from two successive heights by substraction, i.e. $y_1(f) - y_2(f)$, with $B\Delta\tau$ equal to 0.42, 0.84, 1.26, respectively. The data difference enables to filter most of the transient signal in the antenna. The selection of the useful part of the virtual signals is carried out by a time filtering as shown in Fig. 6. The product BT_f of the time

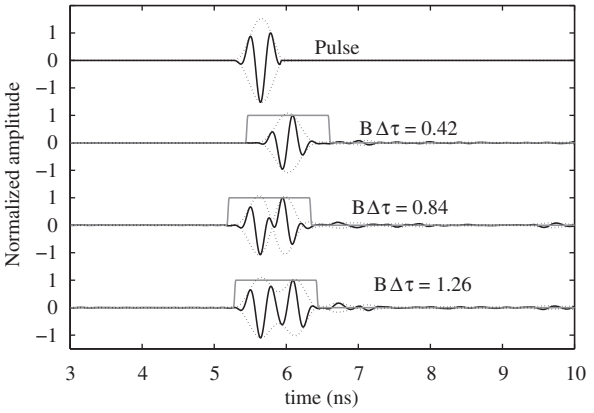

Fig. 6. Backscattered radar pulse from a metal plate and backscattered data from a virtual two-layer medium for the three $B\Delta\tau$ product (0.42, 0.84, 1.26).

Table 1
Relative bias on thickness for three resolving power for the conventional ESPRIT, M-ESPRIT and modified E-ESPRIT algorithms processed on filtered data with uncorrelated echoes.

Algorithms	$B\Delta\tau = 0.42$ (%)	$B\Delta\tau = 0.84$ (%)	$B\Delta\tau = 1.26$ (%)
ESPRIT	62.8	9.2	0.3
M-ESPRIT	7	1.2	0.4
Modified E-ESPRIT	7.5	1.3	0.1

window is fixed at 3.1 for these three experiments, with T_f the duration of the analysis window. This time filtering retains just the two backscattered pulses due to the two interfaces. The echoes coming from the test bed and the transient signal in the antenna are then filtered, as shown in Fig. 6. Due to perfect reflections on the metal plane, the two echoes show the same magnitude (at nearly geometric expansion) as opposed to the simulated data in Section 4.1.

Table 1 presents the relative bias on thickness which is obtained for three values of $B\Delta\tau$ products. As for the simulated results in Section 4.1, the relative bias decreases with increasing $B\Delta\tau$ product. Due to biased TDE, the conventional ESPRIT algorithm delivers the largest error on thickness. The M-ESPRIT and modified E-ESPRIT algorithms give almost the same results because of high SNR. Moreover, in this experiment, the M-ESPRIT and F-ESPRIT methods are equivalent because the noise is considered as Gaussian temporally white.

5. Conclusion

This paper has proposed a generalized version of the conventional ESPRIT algorithm, called M-ESPRIT, which takes the radar pulse and any noise signature into account in the formalism. This algorithm is applied to time delay estimation and aims at improving the performance of the radar-based non-destructive testing methods. As opposed to the previous versions of the algorithm, the proposed M-ESPRIT algorithm enables to process raw data directly without any preprocessing and shows better performance. Besides, this paper has shown that it is better to take account of the radar pulse into the steering vector rather than into the noise metric.

Acknowledgment

The authors are grateful to France's "Pays-de-la-Loire" Regional Council for partially financing this work.

Appendix A. Proof for Eq. (8)

Let us write the GSVD in (4) on each sub-band data as follows:

$$\mathbf{\Gamma}_{sig,1}\mathbf{V}_{sig} = \mathbf{\Sigma}_{o,1}\mathbf{V}_{sig}\mathbf{G} \tag{20}$$

$$\mathbf{\Gamma}_{sig,2}\mathbf{V}_{sig} = \mathbf{\Sigma}_{o,2}\mathbf{V}_{sig}\mathbf{G} \tag{21}$$

where $\mathbf{\Gamma}_{sig,j}$ $(j = 1, 2)$ are the $((N-1)\times N)$ dimensional matrices, defined from the partitioning of the signal covariance matrix, which is expressed as, according to the model in (3)

$$\mathbf{\Gamma}_{sig,j} = \mathbf{\Lambda}_j\mathbf{A}_j\mathbf{\Gamma}_{\mathbf{c}}\mathbf{A}^H\mathbf{\Lambda}^H \tag{22}$$

and $\mathbf{\Sigma}_{o,j}$ and $\mathbf{\Lambda}_j$ are defined in (9) and (10), respectively.

At the first step, the latter definition and the expression of $\mathbf{A}_2$ in (6) are substituted into (21). Some mathematical manipulations lead to the following formula:

$$\mathbf{\Lambda}_2\mathbf{A}_1\mathbf{\Phi}\mathbf{F} = \mathbf{\Sigma}_{o,2}\mathbf{V}_{sig} \tag{23}$$

where $\mathbf{F}$ is the $(K\times K)$ dimensional invertible matrix defined as

$$\mathbf{F} = \mathbf{\Gamma}_{\mathbf{c}}\mathbf{A}^H\mathbf{\Lambda}^H\mathbf{V}_{sig}\mathbf{G}^{-1} \tag{24}$$

Similarly, (20) and (22) are used to obtain the following expression for matrix $\mathbf{A}_1$:

$$\mathbf{A}_1 = \mathbf{\Lambda}_1^{-1}\mathbf{\Sigma}_{o,1}\mathbf{V}_{sig}\mathbf{F}^{-1} \tag{25}$$

At the second step, substituting (25) into (23), gives

$$\mathbf{\Lambda}_2\mathbf{\Lambda}_1^{-1}\mathbf{\Sigma}_{o,1}\mathbf{V}_{sig}\mathbf{F}^{-1}\mathbf{\Phi}\mathbf{F} = \mathbf{\Sigma}_{o,2}\mathbf{V}_{sig}$$

Finally, introducing the $((N-1)\times(N-1))$ dimensional matrix $\mathbf{\Omega}$ defined in (13), the formula for M-ESPRIT (8) is obtained as

$$\mathbf{\Sigma}_{o,2}\mathbf{V}_{sig} = \mathbf{\Omega}\mathbf{\Sigma}_{o,1}\mathbf{V}_{sig}\mathbf{K} \tag{26}$$

with the $(K\times K)$ dimensional matrix $\mathbf{K}$ defined as follows:

$$\mathbf{K} = \mathbf{F}^{-1}\mathbf{\Phi}\mathbf{F} \tag{27}$$

The latter equation shows that $\mathbf{K}$ and $\mathbf{\Phi}$ in (6) are similar matrices, i.e. they have the same eigenvalues. Then, the K eigenvalues of $\mathbf{K}$ can be written as $e^{-2i\pi\Delta f T_k}$ according to (7), and the time delays T_k are retrieved from the argument of these eigenvalues. Contrary to $\mathbf{\Phi}$, $\mathbf{K}$ can be estimated from data (11).

References

[1] R. Roy, T. Kailath, ESPRIT-estimation of signal parameters via rotational invariance techniques, IEEE Trans. Acoust. Speech Signal Process. 37 (7) (1989) 984–995.

[2] F. Gao, A. Gershman, A generalized ESPRIT approach to direction-of-arrival estimation, IEEE Signal Process. Lett. 12 (3) (2005) 254–257.
[3] H. Saarnisaari, TLS-ESPRIT in a time delay estimation, VTC 97, in: Proceedings of the IEEE 47th Vehicular Technology Conference, vol. 3/3, Phoenix, USA, 1997, pp. 1619–1623.
[4] X. Li, R. Wu, An efficient algorithm for time delay estimation, IEEE Trans. Signal Process. 46 (8) (1998) 2231–2235.
[5] A. Lee Swindlehurst, Time delay and spatial signature estimation using known asynchronous signals, IEEE Trans. Signal Process. 46 (2) (1998) 449–462.
[6] C. Le Bastard, V. Baltazart, Y. Wang, J. Saillard, Thin pavement thickness estimation with a GPR by high and super resolution methods, IEEE Trans. Geosci. Remote Sensing 45 (8) (2007) 2511–2519.
[7] X. Dérobert, C. Fauchard, P. Côte, E. Le Brusq, E. Guillanton, J.-Y. Dauvignac, C. Pichot, Step-frequency radar applied on thin road layers, J. Appl. Geophys. 47 (3) (2001) 317–325.
[8] U. Spagnolini, V. Rampa, Multitarget detection/tracking for monostatic ground penetrating radar: application to pavement profiling, IEEE Trans. Geosci. Remote Sensing 37 (1) (1999) 383–394.
[9] S.M. Shrestha, I. Arai, Signal Processing of ground penetrating radar using spectral estimation techniques to estimate the position of buried targets, EURASIP J. Appl. Signal Process. 12 (2003) 1198–1209.
[10] R.O. Schmidt, A signal subspace approach to multiple emitter location and spectral estimation, Ph.D. Thesis, Stanford University, Stanford, Calif, USA, 1981.
[11] J.B. Schneider, Plane waves in FDTD simulations and a nearly perfect total-field/scattered-field boundary, IEEE Trans. Antennas Propag. 52 (12) (2004) 3280–3287.
[12] R. Roy, T. Kailath, Total least squares ESPRIT, in: Proceedings 21th Asilomar Conference on Circuits, Systems and Computers, November 1987.
[13] S. Lambot, E.C. Slob, I. Van Den Bosh, B. Stockbroeckx, M. Vanclooster, Modeling of ground-penetrating radar for accurate characterization of subsurface electric properties, IEEE Trans. Geosci. Remote Sensing 42 (11) (2004) 2555–2568.
[14] H. Yamada, M. Ohmiya, Y. Ogawa, Super resolution techniques for time-domain measurements with a network analyzer, IEEE Trans. Antennas Propag. 39 (2) (1991) 177–183.
[15] D. Grenier, E. Bossé, Decorrelation performance of DEESE and spatial smoothing techniques for direction-of-arrival problems, IEEE Trans. Signal Process. 44 (6) (1996) 1579–1584.